lubricants

MDPI

Article

An Analysis of Flow Field Characteristics Under the Start-Up Condition of a Subway Gearbox

Zhijian Wang [1,2,3,*], Liwei Guo [2], Xinglin Li [3,4], Feng Wu [1] and Jianguo Ye [5]

[1] College of Energy Engineering, Zhejiang University, Hangzhou 310058, China
[2] School of Mechanical Engineering and Rail Transit, Changzhou University, Changzhou 213164, China
[3] Hangzhou Bearing Test and Research Center with Assistance of UNDP/UNIDO, Hangzhou 310022, China; dr.lixinglin@vip.163.com
[4] Machinery Industry Bearing Quality Inspection Center, Hangzhou 310000, China
[5] Suzhou Bearing Factory Co., Ltd., Suzhou 215129, China
* Correspondence: wzj10721180@163.com

Abstract: This study investigates the transient lubrication dynamics of subway gearboxes during acceleration phases through computational fluid dynamics (CFD) modeling. A simplified gearbox model with helical gears, bearings, and oil-guide channels was developed using STAR-CCM+®. Simulations evaluated the effects of three acceleration levels (7.4 m/s^2, 4.4 m/s^2, and 3.2 m/s^2) and three different oil temperatures (−10 °C, 10 °C, and 70 °C) on pressure distribution, churning torque, and oil supply dynamics. The results show that higher acceleration levels intensify transient pressure fluctuations in gear meshing regions and expedite oil supply initiation to bearings. However, the steady-state lubrication performance remains consistent across acceleration magnitudes. Elevated oil temperatures significantly decrease the initial churning torque of a gearbox but increase the steady-state churning torque. There exists an optimal temperature that maximizes the oil supply in the gear meshing zone. In addition, the initial oil supply times for bearings are slightly reduced under lower temperatures. These findings highlight the critical role of transient acceleration and temperature effects in gearbox lubrication optimization, providing insights for enhancing reliability under dynamic operating conditions.

Keywords: subway gearbox; computational fluid dynamics (CFD); start-up; churning torque; volume fraction

check for updates

Received: 8 April 2025
Revised: 12 May 2025
Accepted: 12 May 2025
Published: 15 May 2025

Citation: Wang, Z.; Guo, L.; Li, X.; Wu, F.; Ye, J. An Analysis of Flow Field Characteristics Under the Start-Up Condition of a Subway Gearbox. *Lubricants* **2025**, *13*, 220. https://doi.org/10.3390/lubricants13050220

Copyright: © 2025 by the authors. Licensee MDPI, Basel, Switzerland. This article is an open access article distributed under the terms and conditions of the Creative Commons Attribution (CC BY) license (https://creativecommons.org/licenses/by/4.0/).

1. Introduction

As the core transmission component connecting the traction motor and wheel set, the gearbox's operational reliability critically determines the safe performance of rail vehicles [1,2]. In current rail transit systems, the predominant cause of gearbox failures lies in the insufficient lubrication of internal transmission components. Specifically, under frequent vehicle acceleration, starting, and stopping conditions, gears, bearings, and other critical parts often fail to receive timely oil supply. This deficiency impedes the formation of stable oil films between meshing gears and bearing surfaces, subsequently triggering mechanical failures such as tooth surface wear and bearing seizure [3,4]. Consequently, investigating the dynamic lubrication characteristics of gearbox components under subway acceleration conditions is of significant engineering significance. Optimized lubrication system designs prevent transmission failures and enhance operational maintenance protocols.

Recent research on gearbox splash lubrication characteristics has primarily employed two methodologies—experimental testing and computational simulation. Zhang et al. [5]

developed a novel gearbox oil agitation test platform by modifying the internal geometry of the housing. Through systematic investigations into oil immersion depth, gear speed, and diaphragm configuration, they demonstrated that strategically positioned separators could significantly reduce oil agitation losses and enhance lubrication efficiency. Similarly, Laruelle et al. [6] conducted bench tests on spiral bevel gears, identifying oil immersion depth as the predominant factor influencing agitation losses under varying operational parameters (speed, lubricant properties, and gear geometry). Zhu et al. [7] established a specialized test rig to analyze lubricant flow distribution and bearing–gear lubrication states. By simulating gradient operations (e.g., uphill/downhill) and directional turns via a wedge mechanism, they characterized lubrication performance through temperature monitoring under controlled oil immersion depths and rotational speeds. However, conventional experimental approaches are inherently limited to macroscopic oil distribution analysis, failing to capture high-speed or microscale lubricant flow dynamics, which are essential for the quantitative assessment of gear-bearing lubrication states. To address these limitations, Liu et al. [8] pioneered CFD-based investigations of oil flow patterns in single-stage gearboxes, validating simulation accuracy through experimental comparisons. Liu et al. [9] studied the lubricating oil distribution and agitation loss of the gearbox based on the SPH method, and the oil distribution in the simulation was in good agreement with the test results; however, the agitation loss was quite different from the test results. Stavytskyi et al. [10] analyzed the agitation loss of gears under different working conditions using the CFD method, concluding that the power loss caused by the hydromechanical resistance of gear rotation was consistent with the test data and was used for the actual calculation of high-speed gears. Shao et al. [11] applied the Moving Particle Semi-implicit (MPS) method to evaluate initial oil volume effects on lubrication characteristics, while Shen et al. [12] developed a 3D CFD model for EMU spiral bevel gears, determining that initial oil volume exerted a greater influence on lubricant distribution than speed or temperature variations. Wang et al. [13] and Ma et al. [14] further extended CFD and Smoothed Particle Hydrodynamics (SPH) techniques, respectively, with Ma's team identifying lubrication-risk bearings through flow monitoring surfaces and proposing structural optimizations to mitigate risks. Although these studies employing Finite Volume Method (FVM) and MPS approaches have systematically examined factors such as gearbox geometry, operating speeds, oil temperature, and initial oil volume, their scope remains confined to steady-state operating conditions. Recent efforts by Hu et al. [15,16] on helicopter intermediate gearboxes investigated the tilt angle and directional movement effects on oil distribution and torque, while Liu et al. [17] and Hildebrand et al. [18] explored vibration-induced flow field variations and slope-induced acceleration effects. Nevertheless, existing research predominantly focuses on global gearbox motion analysis, with limited attention being paid to the transient dynamics of internal components—notably, the accelerated rotational behaviors of gears and bearings, which constitute a critical knowledge gap in gearbox lubrication studies under dynamic operational regimes.

To address this critical gap, this study systematically investigates the fluid–structure interaction characteristics within subway gearboxes under accelerated operating conditions through an integrated computational approach. The research framework comprises three key stages. Firstly, a high-fidelity computational model of the subway gearbox was developed, incorporating precise geometrical configurations and multiphase flow parameters. Secondly, multiphysics simulations were conducted through sequential fluid–structure interaction analysis. The oil supply dynamics were quantified by monitoring flow rates in lubrication conduits, which were subsequently applied as boundary conditions for bearing lubrication simulations. Thirdly, the interdependent effects of acceleration levels and oil temperature variations were rigorously evaluated, with particular emphasis on

their impacts on both macroscopic flow field patterns and microscale bearing lubrication performance.

2. CFD Model Setup

2.1. Geometry

To enhance simulation efficiency, the gearbox geometry was simplified by omitting components with negligible effects on lubricant dynamics. As illustrated in Figure 1, the simplified model comprises a gearbox housing, a pair of helical gears, bearings, and oil-guide channels. The labeled oil-guide devices (A, B, C, and D) correspond to their respective bearing positions. During operation, lubricant is entrained by the driven gear's rotation to lubricate the gear surfaces. A portion of the oil splashes into the guide channels and subsequently flows into the bearings.

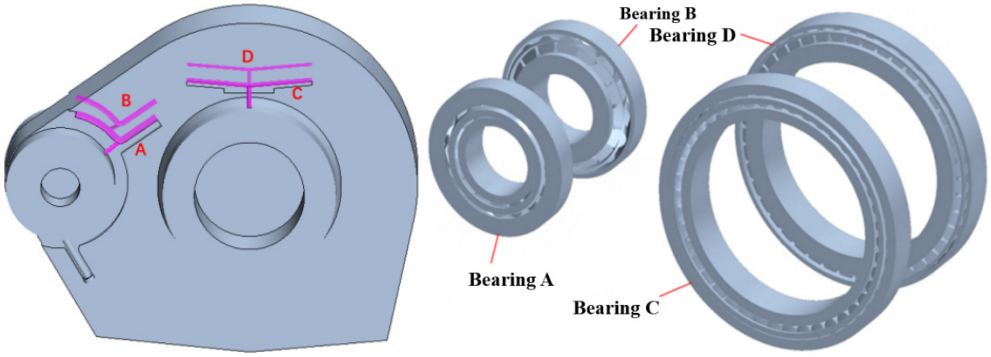

Figure 1. Simplified model of a subway gearbox [13].

2.2. Meshing

The fluid domain mesh of the gearbox and bearings, generated using the overset mesh technique in STAR-CCM+®2019.1 (14.02.010-R8), ensures structural integrity and computational stability (Figure 2). To address the challenge of excessive grid counts in the tight gear meshing region, a scaling method [19] was employed to enlarge gear clearances while preserving flow characteristics. The gearbox domain utilizes a polyhedral mesh with local refinement (3 mm cell size in critical regions versus 5 mm elsewhere), yielding a total of 11.69 million cells. For bearings, trimmed meshes were adopted with localized encryption (1.5 mm cell size in roller-cage gaps versus 3 mm in other regions). Bearing A and C's meshes contain 3 million and 14 million cells, respectively, balancing resolution and computational cost.

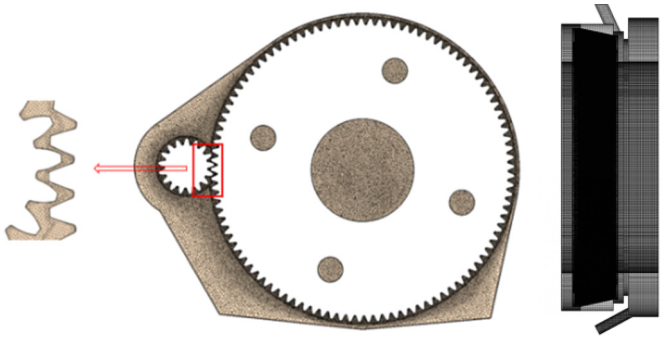

Figure 2. Mesh model.

2.3. Boundary Conditions

The gearbox internal flow field was modeled as a two-phase (air and lubricant) system. The lubricant (75W–90 grade) exhibits temperature-dependent viscosity, as follows: 1.65 Pa·s at −10 °C, 0.391 Pa·s at 10 °C, and 0.0286 Pa·s at 70 °C. Air properties were defined as a density of 1.225 kg/m^3 and a kinematic viscosity of 1.56 mm^2/s. The speeds of the wheels, driving wheels, and driven wheels are represented in Equation (1). The initial oil fill level was set to three times the gear tooth height, as shown in Figure 3, with gear/bearing rotational parameters adopted from [13].

$$\begin{aligned} v &= \frac{2\pi nr}{60} \\ n &= n_1 = n_2 \cdot \frac{z_2}{z_1} \end{aligned} \tag{1}$$

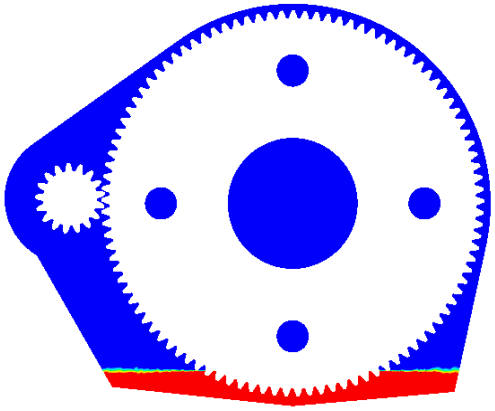

Figure 3. Initial interface of lubricating oil.

v is the running speed of the subway; n is the rotation speed of the subway wheels; n_1 and n_2 are the rotation speeds of the driven wheel and the driving wheel, respectively; and z_1 and z_2 are the number of teeth of the driven wheel and the driving wheel, respectively.

2.4. Solving Process and Algorithm Optimization

Figure 4 shows the flow diagram and the fluid domain model of the transmission bearing, which is divided into the following two steps:

(1) Gearbox Simulation: Determine the flow field characteristics, agitation torque, and flow rates through the oil-guide channels.
(2) Bearing Simulation: Apply the calculated channel flow rates as inlet boundary conditions to analyze the lubricant volume fraction within the bearings.

It should be noted that in order to reduce computational time, the acceleration values were set to 7.4 m/s^2, 4.4 m/s^2, and 3.2 m/s^2. Consequently, for a target steady-state velocity of 80 km/h, the corresponding acceleration times are theoretically determined as 3, 5, and 7 s, respectively. The numerical models for the gearbox and bearing were executed in parallel using 20 processes on a 13th Gen Intel® Core™ i7-13700KF processor (3.40 GHz) with 128 GB RAM. The computational results under modified acceleration conditions are as follows: 3 s acceleration to 80 km/h: ~1100 h for the gearbox and ~400 h for the bearing; 5 s acceleration to 80 km/h: ~1600 h for the gearbox and ~700 h for the bearing; 7 s acceleration to 80 km/h: ~2000 h for the gearbox and ~1000 h for the bearing.

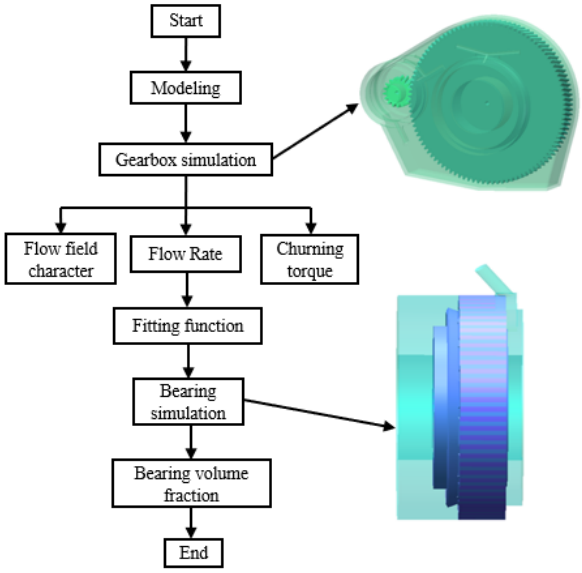

Figure 4. The flowchart of numerical simulation.

3. Results and Discussion

3.1. Effect of Gear Acceleration

Figure 5 shows the cross-sectional pressure distribution of the gearbox during acceleration to 80 km/h at 7.4 m/s^2, 4.4 m/s^2, and 3.2 m/s^2, followed by 2 s of constant-speed operation at an oil temperature of 70 °C. During the initial start-up phase, the internal pressure distribution remained uniform across all acceleration conditions. However, significant pressure differences were observed in the gear meshing area—approximately 3500 Pa at 7.4 m/s^2, 2000 Pa at 4.4 m/s^2, and 1000 Pa at 3.2 m/s^2. These differences arise because higher initial accelerations generate greater gear line velocities, driving rapid lubricant displacement and increased flow rates in the meshing region. As the gears reached peak speed, pressure differences in the meshing region diverged inversely with acceleration—3500 Pa at 7.4 m/s^2, 4500 Pa at 4.4 m/s^2, and 8000 Pa at 3.2 m/s^2. This reversal occurs because higher accelerations cause centrifugal forces to fling most oil toward the gearbox's left wall (Figure 6), reducing oil supply to the meshing area (Figure 7) and thereby lowering pressure differences. After stabilizing at peak speed for 2 s, both pressure differences and lubricant distribution in the meshing area converged to similar levels.

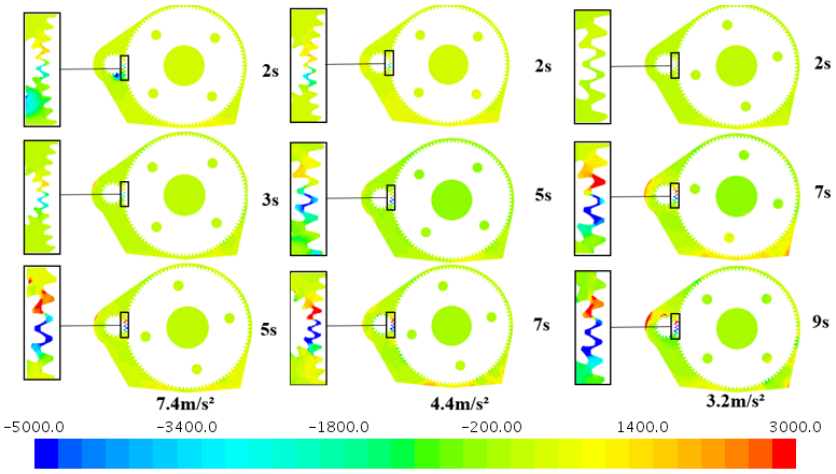

Figure 5. Pressure distribution of the gearbox cross-section at different accelerations.

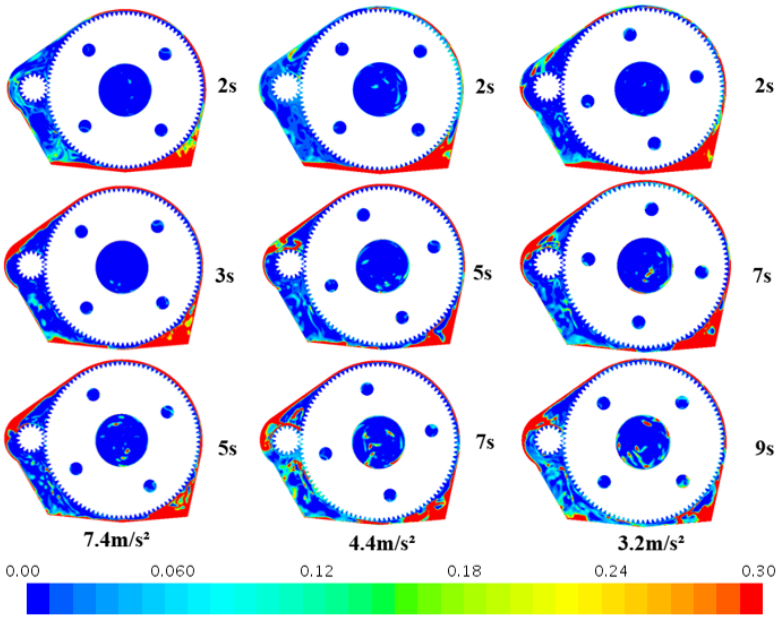

Figure 6. Flow field of the gearbox cross-section at different accelerations.

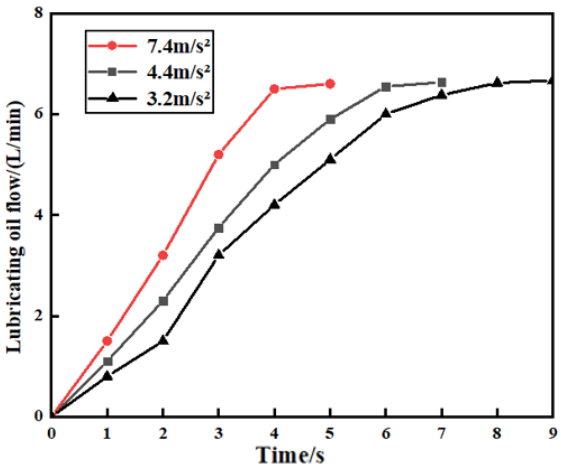

Figure 7. Flow rate in the gear meshing area at different accelerations.

Figure 8 compares the churning torque of the gear under different accelerations. During acceleration, higher accelerations produced larger churning torque values. However, once the gear transitioned to steady-speed operation, the torque stabilized to nearly identical levels across all acceleration conditions, indicating that acceleration primarily impacts transient dynamics rather than steady-state performance.

Figure 9 shows the transition in supply oil behavior under different acceleration levels. From Figure 9, it can be found that bearings initiate oil supply earlier under greater acceleration—with acceleration times of 3, 5, and 7 s, oil supply begins at 0.9 s, 1 s, and 1.2 s, respectively. During acceleration, faster growth rates in oil supply are observed with higher acceleration. For instance, under a 3 s acceleration, Bearing A stabilizes its oil supply in 2 s and Bearing C in 1.5 s, whereas a 5 s acceleration extends stabilization times to 4 s for Bearing A and 2.5 s for Bearing C. Further reducing acceleration to 7 s prolongs stabilization to 6 s for Bearing A and 4 s for Bearing C. Despite these dynamic variations, all bearings ultimately converge to a consistent steady-state oil supply range, demonstrating that acceleration impacts transient responsiveness but not final equilibrium.

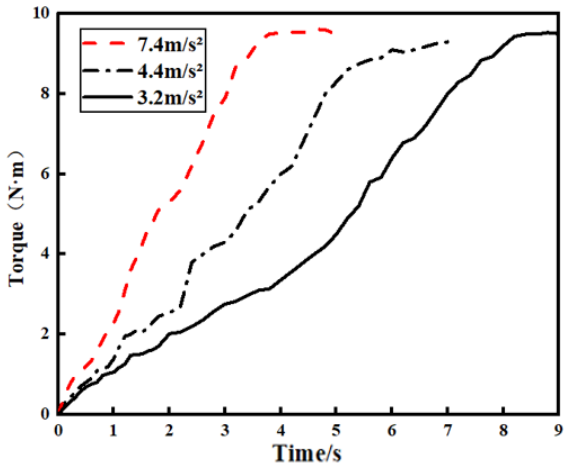

Figure 8. Churning torque of the gear at different accelerations.

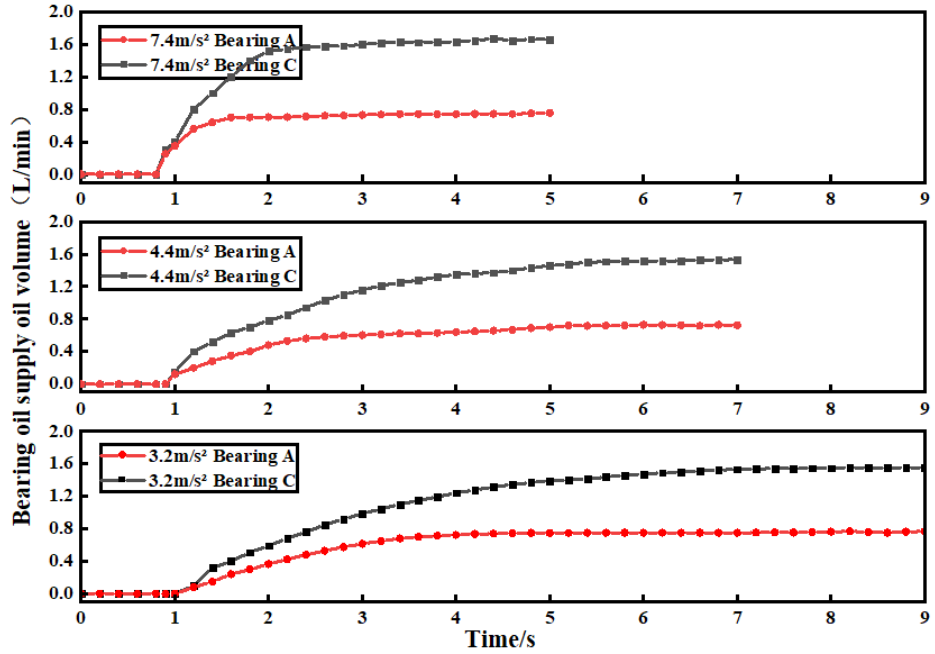

Figure 9. Variation in bearing supply oil volume at different accelerations.

Figure 10 illustrates the oil volume fraction within bearings under different acceleration levels. A low-volume fraction risks direct contact between bearing components (e.g., inner/outer rings and rollers), increasing friction and wear. From Figure 10, it can be revealed that under a 3 s acceleration (highest acceleration), oil volume fractions begin rising at 1.8 s, stabilizing at 2.64% for Bearing C and 0.91% for Bearing A. With a 5 s acceleration, oil supply initiates at 2.2 s, reaching 2.63% (C) and 0.9% (A), while a 7 s acceleration delays initiation to 2.6 s, stabilizing at 2.58% (C) and 0.92% (A). These results demonstrate that higher accelerations shorten oil supply initiation time (e.g., 1.8 s vs. 2.6 s) and enhance transient lubrication efficiency. However, final oil volume fractions remain nearly identical across acceleration levels (C: ~2.6%; A: ~0.9%), indicating that steady-state lubrication depends on oil supply capacity rather than acceleration magnitude. However, it should be noted that in real-world applications, acceleration is relatively low and the acceleration time is relatively long, at around 20 s. As a result, the bearing will experience prolonged periods of oil starvation and frequent start–stops may lead to the wear failure of the bearing.

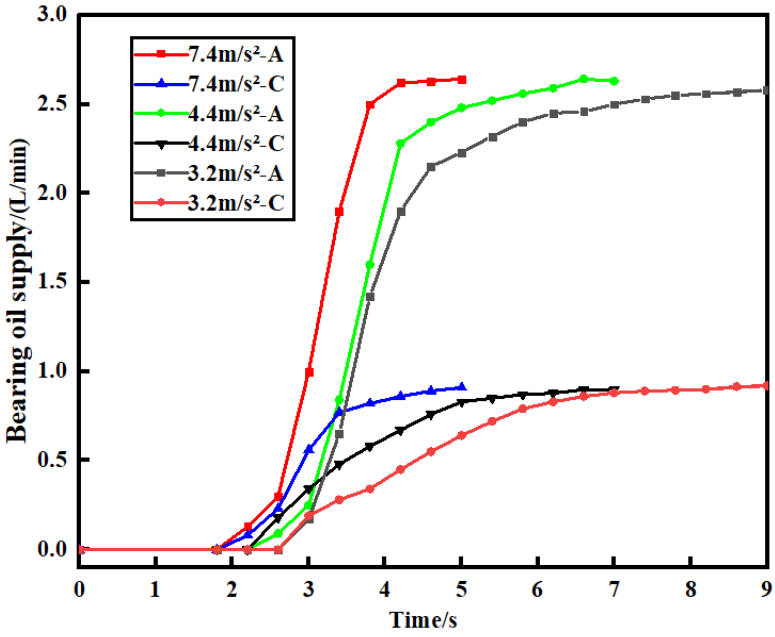

Figure 10. Oil volume fraction of Bearings A and C at different accelerations.

3.2. Effect of Oil Temperature

Figures 11–13 depict the evolution of pressure contours, flow field distribution, and lubricating oil volume in a gearbox under oil temperatures of −10 °C, 10 °C, and 70 °C, with an acceleration time of 3 s. In the initial phase, overall pressure distribution remains uniform across all temperatures, yet localized pressure differences in the gear meshing region intensify with temperature (e.g., they are highest at 10 °C). This is because more lubricating oil is entering into the meshing area at 10 °C. When the temperature is lower, the viscosity of the oil is larger and most of the oil is kept at the bottom of gearbox. However, if the temperature is higher, the viscosity of the oil is smaller and most of the oil is splashed onto the gearbox wall surface. As time progresses, the same trend is exhibited, as shown in Figures 11 and 12. Ultimately, at 10 °C, the gear meshing area has the highest amount of lubricant oil.

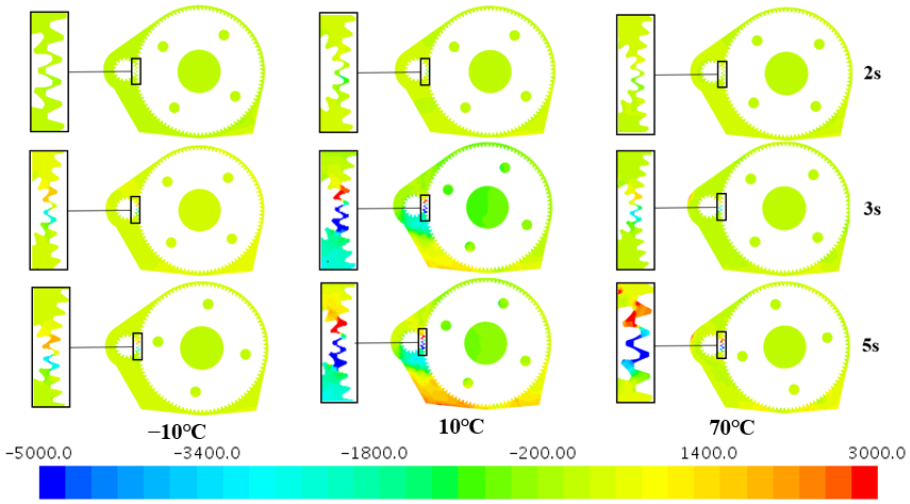

Figure 11. Pressure field of the gearbox cross-section at different temperatures.

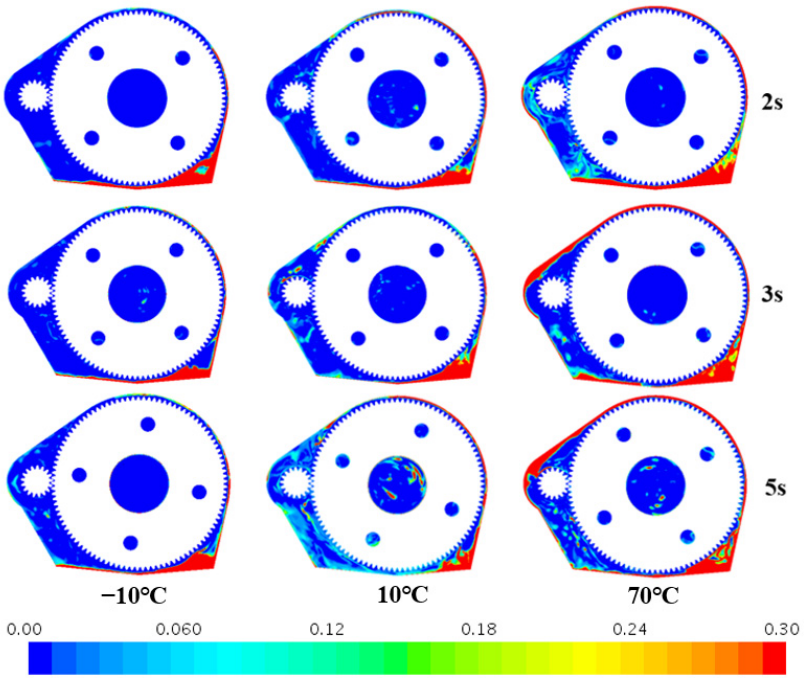

Figure 12. Flow field of the gearbox cross-section at different temperatures.

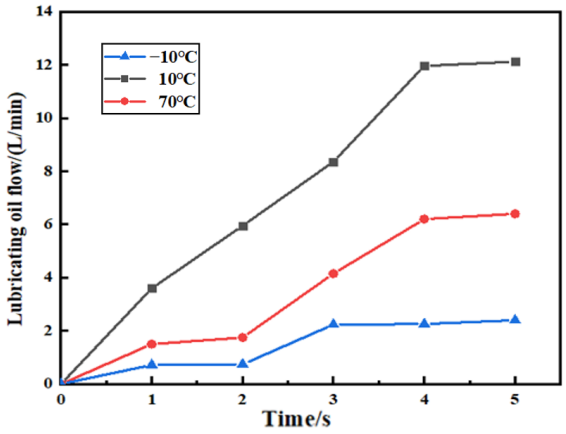

Figure 13. Flow rate in the gear meshing area at different temperatures.

Figure 14 reveals the effect of temperature on churning loss. It can be found that churning torque initially increases and then stabilizes from acceleration to steady state for all temperatures. However, the lower the temperature, the larger the churning loss during the start-up phase. This is because, during initial start-up, the lubricant oil is deposited at the bottom of the gearbox and lower temperatures result in a higher viscosity, leading to increased agitation torque. Over time, as the oil gradually distributes within the gearbox, higher temperatures facilitate broader oil dispersion into the gearbox, thereby further elevating the torque. Consequently, the churning torque is highest under steady-state conditions at 70 °C, which aligns with Liu Hua's experimental findings [20].

Figure 15 shows the variation in bearing supply oil volume at different temperatures. It can be found that across all temperature conditions, the oil supply exhibits an initial rapid increase followed by stabilization. Temperature significantly impacts both the start-up performance and final stable values of the lubrication system. At −10 °C, the oil supply grows most slowly, with a delayed initial supply time of approximately 2 s and a low stable value of 0.04–0.05 L/min for Bearing C, due to increased lubricant viscosity and reduced fluidity under low temperatures. When the temperature rises to 10 °C, the initial

supply time shortens to 1 s and the stable value increases to 0.3–0.4 L/min for Bearing C, reflecting improved fluidity as viscosity moderates. At 70 °C, the system achieves optimal performance—the initial supply time drops to 0.8 s and the oil supply rapidly climbs to a high stable value of 1.6–2.0 L/min for Bearing C, benefiting from reduced viscosity and enhanced flow under elevated temperatures. In addition, Bearing A (red curve) and Bearing C (gray curve) share similar trends across temperatures, and Bearing A consistently maintains slightly higher stable oil supply values because of the different structural or lubrication channel designs. However, as shown in Figure 16, the final lubricant volume fraction inside Bearing A is higher than that in Bearing C, which is attributed to Bearing A's smaller size. Additionally, the initial oil supply times for Bearings A and C are slightly reduced under varying temperatures. This is because in low-temperature conditions, although the oil supply at the inlet starts more slowly, once it enters the bearing chamber, it is rapidly carried into the bearing interior. In contrast, under high temperatures, the lubricant first flows along the wall to the bottom of the bearing chamber and is only drawn into the bearing interior after accumulating to a certain volume, as depicted in Figure 17.

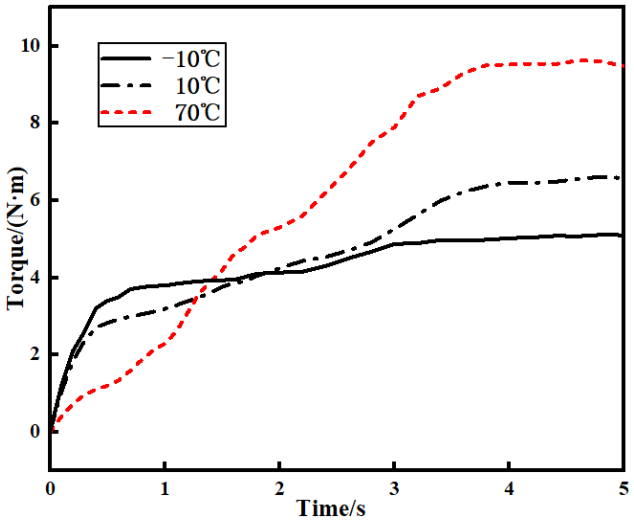

Figure 14. Churning torque of the gear at different temperatures.

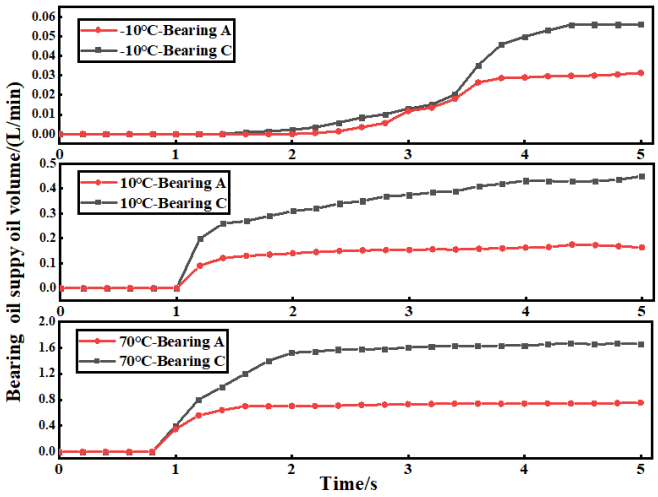

Figure 15. Variation in bearing supply oil volume at different temperatures.

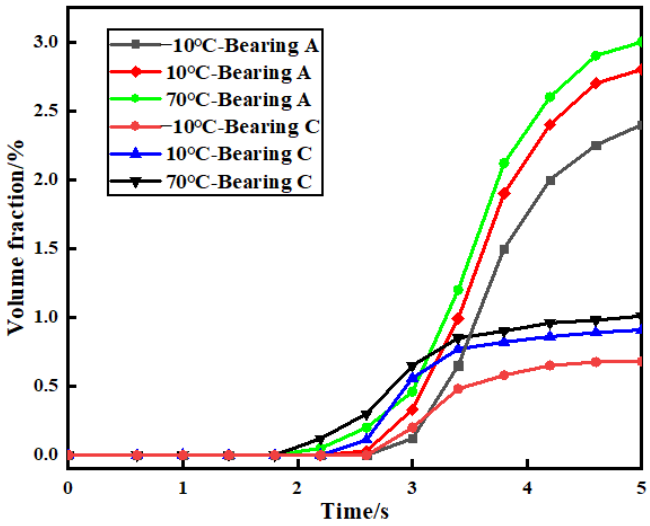

Figure 16. Oil volume fraction of Bearings A and C at different temperatures.

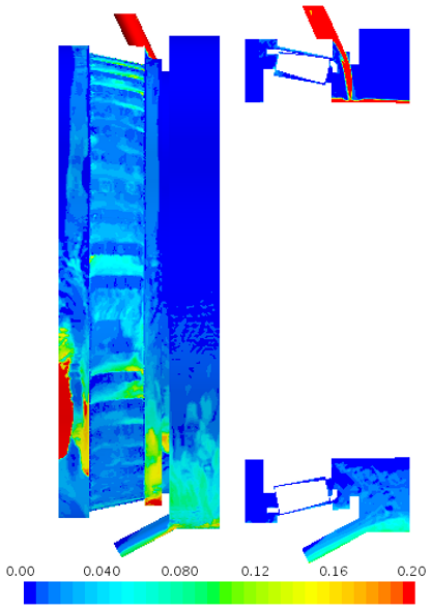

Figure 17. Flow of lubricating oil in bearing chamber.

4. Conclusions

In this study, a transient fluid–structure interaction framework was established to systematically investigate lubrication dynamics in subway gearboxes under accelerated start-up conditions. The computational model integrated overset meshing techniques with multiphase flow analysis. The effects of acceleration magnitude and oil temperature variations on pressure distribution, lubricating oil distribution, and churning torque characteristics were rigorously evaluated through three-phase simulations. The key findings are summarized as follows:

(a) During acceleration phases, higher gear acceleration (7.4 m/s^2 vs. 3.2 m/s^2) induces greater initial pressure differentials (3500 Pa vs. 1000 Pa) in gear meshing regions due to rapid lubricant displacement. However, this relationship reverses at steady-state operation, where lower acceleration preserves higher meshing zone pressure (8000 Pa at 3.2 m/s^2 vs. 3500 Pa at 7.4 m/s^2) through optimized oil retention.

(b) Higher accelerations enhance transient lubrication efficiency of the gear meshing area and the bearings. However, the steady-state performance of the gear meshing area

and the bearings remains consistent across conditions. Therefore, acceleration governs transient dynamics but not equilibrium lubrication.

(c) Temperature critically modulates lubrication dynamics, whereby lower temperatures delay oil supply initiation and restrict bearing flow due to high viscosity, while elevated temperatures accelerate distribution but reduce meshing area retention. Optimal meshing oil accumulation occurs at moderate temperatures, balancing viscosity and flow efficiency.

(d) Although oil temperature influences the initial time required for a lubricant to reach bearing lubrication channels, the final arrival time into the bearing interior just slightly decreases across temperature conditions.

Author Contributions: Conceptualization: Z.W., X.L. and F.W.; methodology: Z.W.; software: L.G.; formal analysis: L.G.; investigation: J.Y.; writing—original draft preparation: Z.W. and L.G.; writing—review and editing: X.L. and F.W.; visualization: J.Y. All authors have read and agreed to the published version of the manuscript.

Funding: The funding for this study is provided by "Pioneer" and "Leading Goose" R&D Program of Zhejiang (Grant No. 2024C01038).

Data Availability Statement: The original contributions presented in this study are included in the article. Further inquiries can be directed to the corresponding author.

Acknowledgments: The funding for this study is provided by "Pioneer" and "Leading Goose" R&D Program of Zhejiang (Grant No. 2024C01038). The authors express their appreciation for the resources received from Changzhou University's High Performance Computation Laboratory.

Conflicts of Interest: Authors Zhijian Wang and Xinglin Li were employed by the company Hangzhou Bearing Test and Research Center. Author Jianguo Ye was employed by the company Suzhou Bearing Factory Co., Ltd. The remaining authors declare that the research was conducted in the absence of any commercial or financial relationships that could be construed as a potential conflict of interest.

References

1. He, Q.; Li, A.; Zhang, J.; Zhang, J.; Ma, J. The development trendof high speed train bearings. *J. Xuzhou Inst. Technol. (Nat. Sci. Ed.)* **2012**, *27*, 58–64.
2. Yang, S.; Wang, X.; Chen, C.; Liu, S. Research status and trend of gearbox design of high-speed EMUs. *Mach. Tool Hydraul.* **2021**, *49*, 173–179.
3. Luo, Z.; Zhang, H. Failure analysis of transmission gears of gearboxes in metro vehicles. *Harbin Railw. Sci. Technol.* **2023**, *4*, 27–31.
4. Cheng, X. Analysis and treatment of typical faults of Zhengzhou metro vehicle gearbox. *Urban Rail Transit Res.* **2022**, *25*, 225–228.
5. Zhang, L.; Wang, B.; Zhou, L.; Wang, J. Experimental design and analysis of oil stirring loss bench for gear oil stirring loss of oil-immersed lubrication reducer. *J. Yancheng Inst. Technol. (Nat. Sci. Ed.)* **2024**, *37*, 67–72.
6. Laruelle, S.; Fossier, C.; Changenet, C.; Ville, F.; Koechlin, S. Experimental investigations and analysis on churning losses of splash lubricated spiral bevel gears. *J. Mech. Ind.* **2017**, *18*, 412. [CrossRef]
7. Zhu, H.; Zhao, J.; Sun, Q.; Zheng, Q.; Liu, S.; Yin, S.; Zheng, Q.; Huo, Y. Design and study of gearbox splash lubrication test bench. *Mech. Des.* **2019**, *36*, 113–116.
8. Liu, H.; Jurkschat, T.; Lohner, T.; Stahl, K. Detailed Investigations on the Oil Flow in Dip-Lubricated Gearboxes by the Finite Volume CFD Method. *Lubricants* **2018**, *6*, 47. [CrossRef]
9. Liu, H.; Arfaoui, G.; Stanic, M.; Montigny, L.; Jurkschat, T.; Lohner, T.; Stahl, K. Numerical modelling of oil distribution and churning gear power losses of gearboxes by smoothed particle hydrodynamics. *Proc. Inst. Mech. Eng. Part J J. Eng. Tribol.* **2019**, *233*, 74–86. [CrossRef]
10. Stavytskyi, V.; Bashta, O.; Nosko, P.; Tsybrii, Y. Determination of Hydrodynamic Power Losses in a Gearing. *Acta Mech. Autom.* **2022**, *16*, 1–7. [CrossRef]
11. Shao, S.; Zhang, K.; Yao, Y.; Liu, Y.; Gu, J. Investigations on lubrication characteristics of high-speed electric multiple unit gearbox by oil volume adjusting device. *J. Zhejiang Univ.-Sci. A* **2022**, *23*, 1013–1026. [CrossRef]
12. Shen, L.; Zhu, Y.; Shao, S.; Zhou, H.; Wang, Z. Research on Splash Lubrication Characteristics of a Spiral Bevel Gearbox Based on the MPS Method. *Lubricants* **2023**, *11*, 520. [CrossRef]

13. Wang, Z.; Guo, L.; Zhou, Z.; Guo, R.; Zhu, L. Flow field analysis and optimization of oil guide structure of metro gearbox splash lubrication. *J. Railw. Sci. Eng.* **2025**, 1–12. [CrossRef]
14. Ma, Y.; Zhan, D.; Liu, J. Improvement of gearbox lubrication structure based on SPH algorithm. *Constr. Mach.* **2022**, *53*, 27–33+8.
15. Hu, X.; Li, P.; Wu, M. Influence of the Dynamic Motion of a Splash-Lubricated Gearbox on Churning Power Losses. *Energies* **2019**, *12*, 3225. [CrossRef]
16. Hu, X.; Jiang, Y.; Luo, C.; Feng, L.; Dai, Y. Churning power losses of a gearbox with spiral bevel geared transmission. *Tribol. Int.* **2019**, *129*, 398–406. [CrossRef]
17. Liu, Y.; Zhang, K.; Shao, S.; Xiang, H.; Ye, Z. Influence of vibration on the lubrication effect of a splash-lubricated gearbox. *J. Zhejiang Univ.-Sci. A* **2024**, *25*, 324–339. [CrossRef]
18. Hildebrand, L.; Dangl, F.; Sedlmair, M.; Lohner, T.; Stahl, K. CFD analysis on the oil flow of a gear stage with guide plate. *Forsch Ingenieurwes* **2022**, *86*, 395–408. [CrossRef]
19. Lu, F.; Wei, K.; Wang, M.; Li, M.; Bao, H. Oil film deposition characteristics and judgment of lubrication effect of splash lubricated gears. *J. Mech. Sci. Technol.* **2023**, *37*, 2383–2393. [CrossRef]
20. Liu, H.; Jurkschat, T.; Lohner, T.; Stahl, K. Determination of oil distribution and churning power loss of gearboxes by finite volume CFD method. *Tribol. Int.* **2017**, *109*, 346–354. [CrossRef]

Disclaimer/Publisher's Note: The statements, opinions and data contained in all publications are solely those of the individual author(s) and contributor(s) and not of MDPI and/or the editor(s). MDPI and/or the editor(s) disclaim responsibility for any injury to people or property resulting from any ideas, methods, instructions or products referred to in the content.